Inter- and intra-domain functional redundancy in the rumen microbiome during plant biomass degradation

Andrea Söllinger[1,2*], Alexander Tøsdal Tveit[3], Morten Poulsen[4], Samantha Joan Noel[4], Mia Bengtsson[2], Jörg Bernhardt[2], Anne Louise Frydendahl Hellwing[4], Peter Lund[4], Katharina Riedel[2], Christa Schleper[1], Ole Højberg[4], Tim Urich[2*]

[1] Department of Ecogenomics and Systems Biology, University of Vienna, Althanstraße 14, 1090 Vienna, Austria

[2] Institute of Microbiology, University of Greifswald, Felix-Hausdorff-Straße 8, 17487 Greifswald, Germany

[3] Department of Arctic and Marine Biology, UiT, The Arctic University of Norway, Hansine Hansens veg 18, 9019 Tromsø, Norway

[4] Department of Animal Science, Aarhus University, Blichers Alle 20, 8830 Tjele, Denmark

*corresponding author, Institute of Microbiology, Felix-Hausdorff-Straße 8, 17487 Greifswald, Germany; Tel.: +49 (0)3834 420 5904; E-Mail: tim.urich@uni-greifswald.de

Email addresses. Andrea Söllinger, andrea.soellinger@univie.ac.at; Alexander Tøsdal Tveit, alexander.t.tveit@uit.no; Morten Poulsen, mpou@teknologisk.dk; Samantha Joan Noel, samantha.noel@anis.au.dk; Mia Bengtsson, mia.bengtsson@uni-greifswald.de; Jörg Bernhardt, Joerg.Bernhardt@uni-greifswald.de; Anne Louise Hellwing, annelouise.hellwing@anis.au.dk; Peter Lund, peter.lund@anis.au.dk; Katharina Riedel, riedela@uni-greifswald.de; Christa Schleper, christa.schleper@univie.ac.at; Ole Højberg, ole.hojberg@anis.au.dk; Tim Urich, tim.urich@uni-greifswald.de

Abstract

Background: Ruminant livestock is a major source of the potent greenhouse gas methane (CH_4), produced by the complex rumen microbiome. Using an integrated approach, combining quantitative metatranscriptomics with gas- and volatile fatty acid (VFA) profiling, we gained fundamental insights into temporal dynamics of the cow rumen microbiome during feed degradation.

Results: The microbiome composition was highly individual and remarkably stable within each cow, despite similar gas emission and VFA profiles between cows. Gene expression profiles revealed a fast microbial growth response to feeding, reflected by drastic increases in microbial biomass, CH_4 emissions and VFA concentrations. Microbiome individuality was accompanied by high inter- and intra-domain functional redundancy among pro- and eukaryotic microbiome members in the key steps of anaerobic feed degradation. Methyl-reducing but not CO_2-reducing methanogens were correlated with increased CH_4 emissions during plant biomass degradation.

Conclusions: The major response of the rumen microbiome to feed intake was a general growth of the whole community. The high functional redundancy of the cow-individual microbiomes was possibly linked to the robust performance of the anaerobic degradation process. Furthermore, the strong response of methylotrophic methanogens is suggesting that they might play a more important role in ruminant CH_4 emissions than previously assumed, making them potential targets for CH_4 mitigation strategies.

Keywords: metatranscriptomics, methane, rumen, microbiome, carbohydrate active enzymes, volatile fatty acids, methanogenesis, archaea, *Methanomassiliicoccales*

Background

Ruminant animals are the dominant large herbivores on Earth. Their evolutionary success is partly due to their tight symbiotic associations with commensal microorganisms (their microbiome) that enables them to utilise otherwise indigestible plant biomass as food sources [1]. Since their domestication in the Holocene, ruminants, in particular cows, have provided humankind with various important goods. However, agricultural farming of cows is also a major source of the potent greenhouse gas (GHG) methane (CH_4), having a global warming potential 28 times higher than carbon dioxide [2].

Cows possess a complex digestive system including a four-compartment stomach, with the largest compartment being the rumen [3], a big anaerobic fermentation chamber harbouring the complex microbiome responsible for the anaerobic degradation of ingested plant biomass. During microbial hydrolysis and fermentation of plant fibres volatile fatty acids (VFA) are produced, which serve as the main energy source of the animal [4]. A prominent end-product of microbial degradation is CH_4, produced by methanogenic Archaea. Individual cows, respectively their symbiotic methanogens, produce up to 500 L of CH_4 per day [5], making ruminant livestock one major anthropogenic CH_4 source [6]. Due to an increasing human world population, milk and meat demands are expected to double by 2050 [7], making the development of sustainable and productive animal farming systems a major challenge in agriculture [8]. CH_4 mitigation strategies are not only of ecological, but also of economic importance as ruminant CH_4 emissions represent an energy loss of 2 – 12 % for the animal [5, 8].

Since the times of the pioneering work of Hungate and others [9, 10, 11, 12], microbiologists have made large efforts to understand the structure-function relationships in the complex rumen microbiome, identifying the microorganisms that participate in certain steps of the anaerobic degradation pathway. More recently, the application of cultivation-independent molecular techniques has helped to uncover the high diversity of bacteria, archaea and eukaryotes residing in the rumen and factors affecting community composition (e.g. [13]). In addition, the usage of meta-

omics techniques has paved the way for a better understanding of the rumen ecosystem and the microbial metabolic potential and activity in the rumen (reviewed by [14]). These studies have revealed differences in rumen microbiome structure between low and high CH_4 emitting cows (e.g. [15, 16]) and the effects of different diets on ruminant CH_4 emissions (e.g. [17, 18, 19]). New insights were also gained by identification of new members of functional groups e.g. new fibrolytic and methanogenic community members [20, 21, 22, 23, 24]. Furthermore, the importance of diurnal microbiome dynamics for the understanding of VFA, H_2 and CH_4 production in the rumen was pointed out recently [25].

Despite these major advances, a holistic understanding of the rumen microbiome is still lacking, including answers to rather simple questions such as "who is doing what and when during feed degradation?". Such a fundamental understanding of the rumen ecosystem, as it was proposed by Hungate already in the early 1960s [11], can help to specifically manipulate the rumen microbiome, to lower CH_4 emissions, without hampering animal productivity, milk and meat quality or being harmful to the animal [14, 26].

To obtain a more comprehensive view on the activity of the rumen microbiome during plant biomass degradation, we performed a longitudinal metatranscriptomics study of microbiome dynamics in lactating cows. We aimed at identifying the active pro- and eukaryotic microbiome members and define their function in the key steps of anaerobic polysaccharide degradation and CH_4 production. We hypothesized that the microbiome exhibits a defined successional pattern, reflecting a cascade of hydrolytic, fermentative and methanogenic steps, accompanied by distinct VFA and gas emission patterns. Based on a previous metatranscriptomic study from our lab [24] and work of others ([27] and references therein), we hypothesized that the recently discovered *Methanomassiliicoccales* are substantial contributors to ruminant CH_4 emissions and will therefore show high activity after ruminant feed intake.

Quantitative metatranscriptomics combined with gas- and VFA profiling enabled linking rumen microorganisms and their transcript profiles to processes. We show extensive inter- and intra-

96 domain functional redundancy among microorganisms at several steps of the anaerobic degradation
97 pathway.
98
99 ## Results
100 **Temporal dynamics of feed digestion.** To investigate the effect of feed intake on CH_4 production by
101 the rumen microbiome we conducted a diurnal feeding experiment over four days and measured
102 CH_4, CO_2 and H_2 emissions of four individual lactating Holstein cows on day four in open circuit
103 respiration chambers (Fig. 1, Supplementary Table S1 and S2). Immediately after the morning
104 feeding, CH_4 and CO_2 emissions approximately doubled (23.4 ± 2.2 L h^{-1} CH_4 and 296.3 ± 11.0 L CO_2 h^{-1}
105) with all animals showing similar dynamics and magnitude of gas production (Fig. 1b). The emissions
106 dropped to before-feeding levels four to six hours after feed intake. H_2 was only detectable during
107 the first hour after feeding started (Fig. 1b) indicative of highly active H_2-producing primary and
108 secondary fermenters providing excessive substrate for hydrogenotrophic methanogens. Similar
109 dynamics in gas emissions were observed during afternoon feeding (Supplementary Figure S1).
110 Likewise, the concentration of VFA in rumen fluid samples increased with peak concentrations
111 measured three and two hours after start of the morning and the afternoon feeding, respectively
112 (Fig. 1c), similar to [25]. However, compared to the gas emission profiles VFA pools were more
113 variable in terms of magnitude and temporal dynamics between the four cows. The immediate
114 accumulation of the fermentation products H_2, CO_2 (i.e. substrates for methanogenesis) and VFA
115 after feeding indicated a fast physiological response of the rumen microbiome to feed intake, with
116 enhanced fermentation rates leading to increased methanogenesis rates. Furthermore, a transient
117 increase of RNA in the rumen fluid was observed, which we consider a proxy for active microbiome
118 biomass. 34.1 ± 6.5, 69.2 ± 10.3, 70.0 ± 13.9 and 37.0 ± 6.3 µg RNA were extracted per gram rumen
119 fluid at t0, t1, t3 and t5, respectively (Fig. 1d). Rumen fluids for VFA quantification and RNA
120 extraction were sampled prior to gas measurements, as it was not possible to sample during

121 respiration chamber measurements. The similar patterns in gases, VFA and RNA profiles reflected a
122 similar behaviour of the cows during the animal feeding trial (Supplementary Table S2).
123 Taken together, GHG emissions, VFA production and RNA content indicated a consistent and fast
124 growth response of the rumen microbiome and strong temporal dynamics on process level (Fig. 1b-d,
125 Supplementary Figure S2) within each individual cow.
126 **Microbiome structure and dynamics**. We generated metatranscriptomes from the rumen fluid RNA
127 using deep Illumina HiSeq paired-end sequencing and analysed the rRNA and mRNA content (Fig. 1,
128 Supplementary Table S3). By taxonomic classification of the small subunit (SSU) rRNA transcripts we
129 investigated if the rumen process dynamics (i.e. gas emissions and VFA production) were reflected in
130 the taxonomic composition of the microbiome. This primer- and PCR-independent approach enables
131 the holistic detection and classification of Eukarya, Bacteria and Archaea, typically not possible via
132 PCR/amplicon-based techniques [28, 29]. The obtained three-domain profiles revealed that all major
133 taxonomic groups known from ruminants were present (Fig. 2a-c, Supplementary Table S4), with
134 eukaryotic, bacterial and archaeal taxa accounting for 25.1 ± 10.5 %, 74.5 ± 10.5 % and 0.3 ± 0.1 % of
135 the SSU rRNA transcripts, respectively. Among the eukaryotes, Ciliates were dominant, accounting
136 for > 70 % of SSU rRNAs in 10 out of 16 metatranscriptomes. The presence of *Entodinium* spp.,
137 *Epidinium* spp. and *Eudiplodinium maggii* and the absence of *Polyplastron multivesiculatum* was
138 indicative of a type B ciliate community as typically found in cattle [30]. Altogether, 155 different
139 bacterial families were detected. Out of these, 32 families were detected in all metatranscriptomes,
140 with the ten most abundant being *Prevotellaceae*, *Succinivibrionaceae*, *Lachnospiraceae*,
141 *Ruminococcaceae*, *Fibrobacteraceae*, *Spirochaetaceae*, *Erysipelotrichaceae*, *Veillonellaceae*
142 (*Negativicutes*), RF16 and *Rikenellaceae*, accounting on average for 93.6 % of all bacterial SSU rRNA
143 reads assigned to family level (Fig. 2c), potentially representing the bovine core microbiome [13]. All
144 archaeal transcripts belonged to methanogens, with *Methanomassiliicoccales* and
145 *Methanobacteriales* being the dominant orders.

Although the same major eukaryotic, bacterial and archaeal taxa were present the rumen fluid microbiomes were highly individual in each cow (Fig. 2d, Supplementary Table S4). For example, the proportion of eukaryotes in the individual rumen fluids varied from 11.6 – 40.9 % of total SSU rRNA transcripts. The two most prominent bacterial families, the *Prevotellaceae* and the *Succinivibrionaceae*, ranged from 21.0 – 66.0 % and 1.6 – 34.4 % of the microbial community composition, respectively. In contrast, their taxonomic composition was remarkably stable over the time course of the experiment (Fig. 2d) and did not show any consistent shifts in the individual cows, as revealed by several methods. Differential gene expression analysis showed no prokaryotic and no eukaryotic SSU rRNAs as differentially expressed at any time, except for three eukaryotic SSU rRNAs (i.e. *Epidinium*, *Eudiplodinium* and unassigned *Litostomata*). The latter were significantly less abundant at t5 compared to t3. Indicator species analysis identified several bacterial and eukaryotic taxa as significantly more abundant at certain time points (Supplementary Figure S3). However, except for the *Trichomonadidae* (*Parabasalia*), a group of flagellated *Protozoa*, which were found to be significantly more abundant at t5, only low abundance eukaryotic taxa were found to be indicators of the later time points. Furthermore, cow identity explained 64% of the variation in community composition (PERMANOVA $p = 0.001$), while time did not explain a significant amount of variation (PERMANOVA $p = 0.06$). Therefore, the strong temporal dynamics in rumen processes could not be explained by a successional shift in the community composition but rather by the strong increase in biomass (as reflected by the RNA content, Fig. 1d).

Analysis of mRNA gene expression profiles corroborated the notion that the observed process dynamics were an effect of overall increase in activities rather than due to an induction of specific microbial taxa or metabolisms. In two time course transitions (t3 vs. t1, t5 vs. t3), no significant differences were detected at all, while one hour after feeding less than 3 % of functional genes were significantly higher expressed (t1 vs. t0). The majority (65 %) fell into the subsystem protein biosynthesis (Fig. 3, Supplementary Table S5), namely transcripts of twelve SSU and 15 large subunit ribosomal proteins and the translation elongation factor G. Additionally, relative abundance of two

RNA polymerase subunit transcripts increased from t0 to t1. Only very few other transcripts, involved in respiration, LPS (Kdo_2-Lipid A biosynthesis) and alanine biosynthesis, biosynthesis of branched-chain amino acids, stress response, DNA repair and VFA production/consumption were significantly more abundant at t1 compared to t0 (Fig. 3, Supplementary Table S5). Our results suggest an immediate upregulation of the protein biosynthesis machinery as the major global response of the microbiome to feed intake.

Quantitative metatranscriptomics. We analysed gene expression patterns of methanogens for successional changes during the experiment, which could explain the strong increase of CH_4 emissions. However, the relative abundance of the methanogenesis-specific mRNAs and SSU rRNA transcripts of methanogen decreased at the time points with highest CH_4 production (Fig. 4a). This pointed to a well-known problem in (meta-)omics approaches [31] i.e. linking relative abundances of taxa or genes/transcripts with biogeochemical processes that are derived from heterogeneous data. We thus calculated transcript abundances per volume of rumen fluid (equation 1) by integrating relative transcript abundance with total RNA concentrations extracted from rumen fluid. Using this quantitative metatranscriptomics approach, the transcript patterns of methanogens mirrored the observed dynamics in ruminant CH_4 emissions, with an increase of transcripts per g rumen fluid one to three hours (t1 and t3) and a decrease five hours after the feeding started (Fig. 4b). Similar effects were observed with gene expression patterns of other, broad cellular functions, e.g. DNA replication (Supplementary Figure S4).

Major players in plant biomass degradation and CH_4 production.

Using this quantitative approach, we conducted a broad, integrative functional screening to identify the major microbial players in three key steps of anaerobic plant biomass degradation: (1) breakdown of complex plant polysaccharides, (2) carbohydrate fermentation to VFA and (3) methanogenesis. We used rumen fluid as proxy to analyse the complete anaerobic degradation cascade, although it has been shown that especially fibrolytic particle-associated communities can differ [32, 33].

198 **Degradation of plant polysaccharides**. A screening for transcripts of carbohydrate active enzymes
199 (CAZymes) revealed that the four dominant CAZyme categories were cellulases, hemicellulases,
200 starch degrading enzymes and oligosaccharide hydrolases, accounting for 77.5 ± 2.1 %
201 (Supplementary Figure S5 & Table S6). We quantified and taxonomically classified these transcripts
202 to reveal their distribution among the rumen microbiome (Fig. 5). Three higher-level bacterial and
203 two eukaryotic taxa were identified as predominantly involved, namely *Prevotellaceace*
204 (*Bacteroidetes)*, *Clostridiales* (*Firmicutes)*, *Fibrobacter*, *Ciliophora* and *Fungi* (*Neocallimastigaceae*).
205 While some of the links were known, e.g. *Fibrobacter* as major producer of cellulases [34], others are
206 providing new insights into the complexity of CAZyme production by rumen microorganisms. For
207 instance, Ciliates produced substantial amounts of hemicellulase and cellulase transcripts, and
208 surprisingly few transcripts encoding starch-degrading enzymes, although they have long been
209 considered as starch degraders [35]. Furthermore, the anaerobic fungi *Neocallimastigaceae*,
210 produced the largest share of cellulase transcripts of all microorganisms. The abundant share of
211 cellulase and hemicellulase transcripts encoded by *Clostridiales* establishes them as another key fibre
212 degrading bacterial group in the rumen [36]. The data also show that *Prevotellaceae* primarily
213 expressed genes encoding oligosaccharide hydrolases, starch degrading enzymes and hemicellulases,
214 but not cellulases. *Firmicutes* appeared to have the broadest capacity for polysaccharide
215 degradation, with equal abundances of CAZyme transcripts in all four investigated categories.
216 However, the *Firmicutes* (*Clostridiales*) comprised several different genera within the
217 *Ruminococcaceae* and *Lachnospiraceae*, whereas *Fibrobacteres* and *Bacteroidetes* were dominated
218 by a single genus, *Fibrobacter* and *Prevotella*, respectively.
219 The taxonomic distribution of CAZymes displayed strong differences between the cows, pointing to
220 the same individuality as observed in the taxonomic composition of the rumen microbiome; e.g.
221 Eukaryotes dominated the cellulase transcript pools in cow 1 and cow 4, whereas in cow 2 and cow 3
222 *Fibrobacteres* and *Firmicutes* cellulase transcripts were equally abundant to *Ciliophora* and *Fungi*
223 cellulase transcripts. Thus, the expression of the different CAZyme categories by three to four

different taxa shows a high functional redundancy for polysaccharide degradation in the rumen microbiome, within and between different domains of life.

VFA production. Acetate, propionate and butyrate were the major VFAs accounting for 60.4 ± 4.9 %, 21.9 ± 3.4 % and 11.6 ± 2.7 % of total VFAs, respectively. VFA concentrations in the rumen fluid increased after feed intake, while the pH dropped (Fig. 1c, Supplementary Table S7). Although no VFA production or absorption rates were measured, it has been shown that VFA concentrations are suitable proxies for production rates [4]. Quantitative metatranscriptomics revealed the presence of transcripts for three complete acetate production pathways from pyruvate, i.e. directly (via pyruvate:ubiquinone oxidoreductase, *pox*B), via acetyl-CoA and via acetyl-CoA and acetyl-P (Supplementary Figure S6). The transcripts were assigned to *Bacteroidetes* (mainly *Prevotella*) and *Firmicutes* (i.e. *Clostridiales* and *Negativicutes*), with transcript levels of *Prevotella* exceeding *Firmicutes* up to 30-times in the acetyl-CoA and acetyl-P pathway (Supplementary Figure S7A and B). In general, *pox*B transcript abundances (direct conversion of pyruvate to acetate) were one to two orders of magnitude lower than abundances of the other pathways (Supplementary Figure S7C), with *Clostridiales pox*B transcripts dominating over those of *Prevotella pox*B in all samples (1.4 – 64 times). Together, these results suggest that *Prevotella* were the dominant acetate producers in this experiment.

Transcript analysis revealed the presence of two distinct pathways for propionate production (Supplementary Figure S8), (1) from succinate (succinate pathway) and (2) from lactate (acrylate pathway). Transcript levels of *Prevotella* again exceeded *Firmicutes* (i.e. *Clostridiales*; up to 20-times), suggesting that *Prevotella* also dominated propionate production (Supplementary Figure S9A). Transcripts for two complete pathways possibly leading to butyrate production were detected within the *Firmicutes,* i.e. the butyrate kinase pathway within *Clostridiales* and the butyryl-CoA:acetate CoA-transferase pathway within *Negativicutes* (Supplementary Figure S8 and S9B). These pathways only differ in the last step, i.e. the conversion of butyryl-CoA to butyrate, which is performed in two steps via butyryl-P by *Clostridiales* and directly by *Negativicutes*. In general, transcript abundances of VFA

production pathway enzymes mirrored the VFA concentration patterns, especially for acetate but to a lesser extend also for propionate and butyrate (Supplementary Figure S6 & S8), with a peak in transcript abundance at t1 or t3 and a subsequent decrease of transcripts at t5. Again, the transcript abundances and their taxonomic distribution showed marked differences between the individual cows. For instance, the abundance of transcripts for acetate production via acetyl-CoA and propionate production assigned to *Bacteroidetes* (mainly *Prevotella*) was much higher in cow 1 compared to the other cows, reflecting the higher relative abundance of *Prevotella* within cow 1. Furthermore, *Negativicutes* (formerly *Veillonellaceae*) had a higher transcriptional activity for acetate production via acetyl-CoA and butyrate production than *Clostridiales* within cow 2 (Supplementary Figure S6 & S8) but not within the other cows.

Methanogenesis. *Methanomassiliicoccales* and *Methanobacteriales* were the two dominant methanogenic orders, accounting for > 99 % of SSU rRNAs. All SSU rRNA transcripts assigned to the *Methanomassiliicoccales* belonged to the GIT clade [37] a sister lineage of *Methanomassiliicoccaceae*. Within the *Methanobacteriales*, the majority of the SSU rRNA transcripts belonged to the genus *Methanobrevibacter*, whereas *Methanosphaera* accounted for up to 13.3 % (mean 6.0 %). Between 2.7% and 24.4 % of *Methanobacteriales* SSU rRNA transcripts could not be assigned on a genus level (mean 15.2 %).

The abundance of SSU rRNA transcripts of both groups followed the CH_4 emission dynamics (Fig. 6a). However, only *Methanomassiliicoccales* showed a strong positive linear correlation ($r_s = 0.75$, $p < 0.001$) and only their SSU rRNAs showed significant differences over time similar to the CH_4 emissions (Fig. 6a). Methyl coenzyme M reductase (Mcr), the enzyme catalysing the last step in methanogenesis is conserved in all methanogenic Archaea. The gene encoding the α-subunit of Mcr, *mcr*A, has thus been established as functional and phylogenetic marker for methanogens [38, 39]. No significant differences in *mcr*A transcript abundance were detected (Fig. 6b).

The specific methanogenesis pathways differ fundamentally between *Methanomassiliicoccales* and *Methanobacteriales* (*Methanobrevibacter* and *Methanosphaera*). *Methanomassiliicoccales* are H_2

276 dependent methylotrophic methanogens reducing methylamines and methanol to CH_4 with H_2 as
277 electron donor [40, 41] In contrast, *Methanobrevibacter* produces CH_4 mainly via the reduction of
278 CO_2 with H_2 as electron donor. *Methanosphaera* in turn produces CH_4 from methanol and H_2 [42]. To
279 identify temporal changes in the type of methanogenesis pathways actively used, we searched for
280 transcripts of key-enzymes in these taxon-specific methanogenesis pathways: (1) Methylamine-
281 specific methyltransferases (*mtMA*), involved in methanogenesis from methylamines by
282 *Methanomassiliicoccales*, (2) Methyl-H_4MPT:HS-CoM methyltransferase (*mtr*A), involved in
283 methanogenesis from H_2 and CO_2 by *Methanobrevibacter* and (3) Methanol-specific
284 methyltransferase transcripts (*mta*B) involved in methanogenesis from methanol by
285 *Methanosphaera* and *Methanomassiliicoccales*. We observed the same pattern for
286 *Methanomassiliicoccales mtMA* transcripts as for the SSU rRNA transcripts, i.e. a strong positive
287 response to the feed intake (Fig. 6c). In contrast, no response of *Methanobrevibacter mtr*A transcript
288 levels was observed. Immediately after feed intake, the abundance of *mta*B transcripts of
289 *Methanosphaera* increased, correlating positively with CH_4 emissions ($r_s = 0.59$, $p < 0.05$) (Fig. 6d),
290 while *Methanomassiliicoccales mta*B transcripts negatively correlated with CH_4 emissions ($r_s = -0.63$,
291 $p < 0.01$). Taken together, these results indicate that only the methyl-reducing methanogens
292 *Methanosphaera* and *Methanomassiliicoccales* responded to feed intake.
293

294 **Discussion**

295 In this study, we used an integrated approach, combining metatranscriptomics with targeted
296 metabolomics (gas and VFA profiling) to holistically investigate the temporal rumen microbiome
297 dynamics during plant biomass degradation in lactating cows.
298 By integrating relative transcript abundances with RNA concentrations, we were able to establish the
299 link between rumen microorganism and their activity to processes such as gas emissions and VFA
300 production. Due to the fast growth response of the microbiome to ruminant feed intake relative
301 transcript abundances, which are commonly used in (meta-)transcriptomics, were not sufficient to

establish this link. Few studies have already applied quantitative metatranscriptomics in marine ecosystems (e.g. [43, 44]), focussing on Bacteria and nutrient cycling. Our study is the first host-associated study aiming to link process data to microbial taxa and functions. Furthermore, our approach is different as we apply total RNA concentrations instead of internal mRNA standards for sizing up metatranscriptomics. This quantitative approach allowed us to assess the temporal dynamics of major bacterial, eukaryotic and archaeal taxa involved in the three key steps of anaerobic plant biomass degradation in the cow rumen.

Our results showed that the microbiome composition was surprisingly stable during feed digestion. The strong increase of ruminant CH_4 emissions after feeding was not related to a microbial community shift as we had hypothesized but to a fast growth response of the whole rumen microbiome. This led to enhanced fermentation rates, reflected by the increase of CO_2, H_2 and VFA concentrations and an associated rise in methanogenesis rates. A similar dynamic of bacterial concentrations (SSU rRNA gene copies per mL rumen fluid) as a response to ruminant feed intake was reported recently [25].

While the rumen microbiomes were stable over time, the individual microbiomes differed substantially between the four cows. Despite strong variation in abundance of bacterial and eukaryotic community members, these microbiomes exhibited similar fermentation characteristics, evidenced by gas output and VFA patterns. This points towards extensive functional redundancy among rumen microbiome members, where multiple microorganisms possess the same functional trait(s) and can replace each other [45, 13]. In fact, we could show high functional redundancy at all three key-steps of anaerobic carbohydrate degradation to CO_2 and CH_4.

Remarkably, inter-domain functional redundancy was widespread among the fibrolytic community, where eukaryotes and bacteria contributed varying amounts of CAZyme transcripts within individual cows. For instance, most cellulase transcripts stemmed from two bacterial (*Fibrobacter* and *Clostridiales*) and two eukaryotic groups (*Neocallimastigaceae* and *Ciliophora*), with the eukaryotes

328 producing the largest share of cellulase transcripts in two out of the four cows. Inter-domain
329 functional redundancy was also observed within hemicellulose, starch and oligosaccharide
330 degradation, with marked differences between individual cows. Our results add to the growing
331 notion that eukaryotic contribution to fibre degradation has been underestimated in the past. Very
332 recent metatranscriptomic work with one individual sample also suggested ciliates and fungi as
333 important for (hemi-)cellulose degradation [21].
334 Host individuality and functional redundancy were also revealed in the second key step of anaerobic
335 plant biomass degradation, i.e. the fermentation of carbohydrates to VFA. Three major, well known
336 VFA producing taxa [46, 47] were identified and their contribution to transcript pools of enzymes
337 involved in VFA production was cow dependent. These taxa, i.e. *Bacteroidetes* (*Prevotella*),
338 *Clostridiales* and *Negativicutes (Veillonellaceae*) produced acetate, propionate and butyrate via
339 different fermentative pathways, of which some where shared among taxa and others were taxon-
340 specific. Although *Prevotella* and *Clostridiales* in general dominated acetate/propionate and butyrate
341 production, respectively, *Negativicutes* contributed substantially to acetate production via acetyl-
342 CoA and butyrate production via the butyryl-CoA:acetate CoA-transferase pathway in cow 2.
343
344 The third and terminal step in anaerobic feed degradation is catalysed by methanogens. Also among
345 these we observed functional redundancy. All detected groups (i.e. *Methanomassiliicoccales*,
346 *Methanobrevibacter* and *Methanosphaera*) are characterised as hydrogenotrophic using H_2 as
347 electron donor [40, 41, 42]. The removal of H_2 is important for the rumen ecosystem and the host
348 because low concentrations of H_2 ensure high fermentation rates and efficient feed digestion [48].
349 The longitudinal experimental setup revealed temporal dynamics in electron acceptor usage within
350 the *Methanomassiliicoccales,* where the fraction of methanol-specific methyltransferase transcripts
351 was much lower immediately after feeding, exhibiting an opposite expression pattern to the
352 methylamine-specific methyltransferases. In turn, it appeared that *Methanosphaera* dominated
353 methanol reduction at these time points, showing once more the redundancy among organisms of

the same functional guild. The root cause for this might be manifold, e.g. due to a higher substrate affinity of *Methanomassiliicoccales* for methylamines as compared to methanol or higher concentrations of methylamines. Alternatively, *Methanosphaera* could outcompete *Methanomassiliicoccales* for methanol under conditions of high H_2 partial pressure. Taken together, the data suggest that the methyl-reducing *Methanomassiliicoccales* and *Methanosphaera* were responsible for the increase of CH_4 emissions immediately after feed intake and not the CO_2-reducing *Methanobrevibacter*. This is surprising, given that CO_2 is a much more abundant methanogenesis substrate than methylamines and methanol. The sources of methylamines, i.e. glycine betaine (from beet) and choline (from plant membranes), and methanol (from the hydrolysis of methanolic side-groups in plant polysaccharides) are well known [49], however the amount of these substrates might vary substantially with different diets. Previous, less temporally resolved work suggested that *Methanobrevibacter* was associated with high CH_4 emissions [14, 49]. However, a comparison of sheep rumen metagenomes and metatranscriptomes indicated that *Methanomassiliicoccales* are very active community members in both high and low CH_4 "emitters", with around 5 times higher abundances in the metatranscriptomes compared to the metagenomes [16]. Furthermore, their transcript abundances were significantly higher in high CH_4 "emitters". Also in cows, it was shown that *Methanomassiliicoccales* can represent the predominant active methanogens [24]. In fact, a need for more research on methyl-reducing methanogens in the rumen was pointed out recently [49], including quantifying their contribution to rumen methane production. Further studies on *Methanomassiliicoccales* and *Methanosphaera* physiology *in vitro* and metabolic interactions with the substrate-providing microorganisms *in situ* might identify novel targets for CH_4 mitigation strategies, such as enzymes of the methyl-reducing pathway or the supply of methylated substrates. Such efforts might complement general methanogenesis inhibitors such as 3-nitrooxypropanol to achieve more efficient methane mitigation [50].

Conclusions

To our knowledge, our study is the first longitudinal integrated meta-omics analysis of the rumen microbiome during plant biomass degradation. It is another step towards a comprehensive system-level understanding of the dynamic rumen ecosystem, as envisioned by Hungate and coworkers already more than 50 years ago [11]. Applying a quantitative metatranscriptomics approach, it enabled the time-resolved link between microbiome structure and function and rumen processes. It revealed a rather simple response to feed intake, namely a general growth of the whole community, without the detection of distinct successional stages during degradation. The cow-individual microbiomes exhibited a surprisingly high functional redundancy at several steps of anaerobic degradation pathway, which can be seen as example for the importance of multi-functional diversity for robustness of ecosystems, similar to what has been found in terrestrial biomes [51]. It furthermore points towards CH_4 mitigation strategies that directly tackle the producers of CH_4, since all other functional guilds show high organismic diversity with individual taxa being replaceable by others.

Methods

Animal feeding trial (Fig. 1a). The animal feeding trial was conducted at the Department of Animal Science, Aarhus University (Denmark). The animal experiments were approved by The Experimental Animal Inspectorate under The Danish Ministry of Justice (journal no. 2008/561-1500). Four rumen-cannulated lactating Holstein dairy cows were fed a typical dairy cow diet containing mainly clover grass and corn silage (Supplementary Table S1 and S2) twice a day in a semi-restrictive way. The cows were in the second parity or later, they were 215 ± 112 (mean ± standard deviation) days in milk, had live weight at 602 ± 20 kg and had a milk yield at 33.5 ± 5.4 kg (Supplementary Table S8). Prior to the sampling, which was conducted over four days, the animals had been fed the respective diet continuously for more than two weeks. Day 1: Cows were fed ad libitum. Day 2: The feed was removed at 4 am, cows were allowed to eat from 7 am to 8 am, and again from 2 pm until 4 am the next day. Rumen fluid was sampled at time points 4 am, 7 am, 8 am and every second hour until 10

406 pm, and with a final sampling at 4 am on day 3. Rumen fluid was randomly sampled from different
407 areas of the rumen, pooled and filtered through sterile filter bags with a pore size of 0.5 mm (Grade
408 Blender Bags, VWR, Denmark). The pH of the rumen liquid samples was directly analysed with a
409 digital pH meter (Meterlab PHM 220, Radiometer, Denmark) and subsamples were frozen at -20°C
410 for VFA analysis and other chemical analysis, or flash-frozen in liquid nitrogen and stored at -80°C for
411 nucleic acid extraction. Day 3: Animals were transferred to custom-built transparent polycarbonate
412 open-circuit respiration chambers (1.45 x 3.90 x 2.45 m) and fed ad libitum. Day 4: The cows were
413 fed like on day 2. CH_4, CO_2 and H_2 were quantified continuously throughout the day.
414 **CH_4, CO_2, H_2 and VFA quantification**. The open-circuit indirect calorimetry based respiration
415 chambers, kept at slight under pressure, measured gas exchange (CH_4, CO_2, O_2, and H_2; Columbus
416 Instruments, Columbus, USA), air flow and feed intake continuously during the experiment as
417 described in detail in [52] and in [53]. VFAs in the rumen liquid samples were quantified using a
418 Hewlett Packard gas chromatograph (model 6890, Agilent Technologies Inc., Wilmington, DE, USA)
419 with a flame ionization detector and a 30-m SGE BP1 column (Scientific Instrument Services, NJ, USA)
420 as described in [54].
421 **Nucleic acid extraction and linear RNA amplification** (Fig. 1a). Nucleic acids were extracted based on
422 the method of [55], and as described in [28]. Extraction buffer and phenol:chloroform (5:1, pH 4.5,
423 ambion), 0.5 mL of each, were added to a lysing matrix E tube (MP Biomedicals) containing
424 approximately 0.25 g of rumen fluid sample. Cells were mechanically lysed using a FastPrep machine
425 (MP Biomedicals, speed 5.5, 30 sec) followed by nucleic acid precipitation with PEG 8000. All steps
426 were performed on ice or at 4°C. Nucleic acids were re-suspended in 50 µL DEPC H_2O and 1 µL of
427 RNaseOUT™ (Thermo Fisher Scientific) was added. 10 µL of nucleic acid extracts were subject to
428 DNase treatment (RQ1 DNase, Promega) and subsequent RNA purification (MEGAclear™ Kit,
429 Ambion). Quantity and quality of RNA was assessed via agarose gel electrophoresis, NanoDrop® (ND
430 1000, peqlab) and Qubit™ (Thermo Fisher Scientific). Absence of DNA in the RNA preparations was
431 verified by PCR assays targeting bacterial SSU rRNA genes and archaeal *mcrA* genes. MessageAmp™

II-Bacterial Kit (ambion) was used according to the manufacturer´s manual to synthesise cDNA (via polyadenylation of template RNA and reverse transcription) and perform in *vitro* transcription on the cDNA to amplify total RNA.

Sequencing and sequence data pre-processing. Illumina HiSeq 2500 paired-end (125 bp) sequencing was performed at the Next Generation Sequencing Facility of the Vienna Biocenter Core Facilities on cDNA. The template fragment size was adjusted that paired sequence reads could be overlapped. We used PRINSEQ lite v. 0.20.4 [56] to apply quality filters and trim the reads (parameters -min_len 180 -min_qual_mean 25 -ns_max_n 5 -trim_tail_right 15 -trim_tail_left 15). SortMeRNA v. 2.0 [57] was used to separate sequence reads into SSU rRNA, LSU rRNA and putative mRNA reads. For more details and results of the initial data processing steps see supplementary Table S3. All computations were performed using the CUBE computational resources, University of Vienna (Austria), or run on the HPC resource STALLO at the University of Tromsø (Norway). Raw sequence data have been submitted to the NCBI Sequence Read Archive (SRA) under the accession numbers SAMN07313968 - SAMN07313983.

Taxonomic classification of SSU rRNA reads. We generated random SSU rRNA subsamples containing 50,000 reads out of all SSU rRNA reads with a length between 200 to 220 bp (45.8 ± 11.5 % of total SSU rRNA reads). These subsamples were taxonomically classified with BLASTN against the SilvaMod rRNA reference database of CREST [58] and analysed with MEGAN [59] v. 5.11.3 (parameters: minimum score 100, minimum support 1, top 2 %, 50 best blast hits). Three domain profiles were visualised with treemaps based on CREST taxonomy. Statistical analyses were done with R [60]; packages: edgeR [61], vegan [62], indicspecies [63], heatmap3 [64].

Analysis of mRNA. All putative mRNA reads were compared against the GenBank nr database using DIAMOND ([65]; v0.7.11, database as of December 2015, CUBE).

CAZzymes. Randomly selected subsamples of 2 million nucleotide reads per dataset were translated into open reading frames (ORFs) of 30 amino acids or longer. The ORFs were screened for protein families using HMMER and reference Hidden Markov Models (HMMER v3.0, against the Pfam

458 database v27; [66]). All database hits with e-values below a threshold of 10^{-4} were counted. Pfam
459 annotations were screened for CAZymes using Pfam models of previously identified CAZymes [67]
460 and additional rumen relevant CAZymes [22] as well as CAZymes added to the Pfam-A database after
461 these publications and summarized into higher categories (Supplementary Table S6). Translated
462 reads assigned to any Pfam model of one of the four most dominant categories i.e. cellulases,
463 hemicellulases, starch degrading enzymes and oligosaccharide hydrolases (Supplementary Figure S5)
464 were extracted and blastp was used to obtain taxonomic information (blastp against the monthly
465 updated nr db 04.2016, CUBE). BLAST tables were imported in MEGAN (parameters: minimum score
466 50, minimum support 1, top 5 %, 25 best blast hits) and further analysed. CAZymes were quantified
467 as described below (equation 1).
468 **VFA.** All mRNA reads assigned to any major taxa involved in the production of VFA, as identified by
469 the SEED analyzer implemented in MEGAN, were subject to further analysis to reconstruct major VFA
470 production (turnover) pathways. These metatranscriptomic libraries were screened for all enzymes
471 (via their respective EC numbers) involved in the production/turnover of acetate, propionate and
472 butyrate, by blastp searches (evalue threshold $1e^{-10}$) using the metatranscriptomic libraries as queries
473 against the UniRef50 database (montly updated, 12.2016, CUBE). The respective enzyme names were
474 derived from the KEGG reference pathways and literature [68, 69]. Heatmaps were constructed in R
475 using quantified data (µg transcripts g^{-1} rumen fluid; equation 1) normalized by the sum of each
476 transcripts over all time-points for each individual cow.
477 **Methanogenesis**. Specific transcripts for methanogenesis were extracted from the DIAMOND
478 annotation files via MEGAN and the implemented SEED analyzer. Assignments were critically
479 manually evaluated and in case of uncertainty blastn was used to verify accuracy and origin of the
480 methanogenesis transcripts as well as of the SSU rRNA transcripts (against the NCBI and Silva
481 databases as of September 2016). Transcripts were quantified (equation 1). Pearson's product-
482 moment correlations and spearman rank correlation coefficients (rho = r_s) between methanogen
483 specific transcripts (pathway specific key transcripts and SSU rRNA transcripts) were calculated and

paired t-test was used to assess temporal differences in transcript abundance (R functions: shapiro.test, cor.test, t.test).

Differential gene expression analysis. mRNA. DIAMOND annotations were imported in MEGAN (parameters: minimum score 40, minimum support 1, top 10 %) and relative abundances of mRNA reads assigned to a SEED function were subject to differential gene expression analysis using edgeR (function: glmFit). Low expressed genes were filtered out and the default TMM method was used to normalize the data. To account for the cow differences a design matrix was constructed prior to the analysis to account for our experimental design and correct for batch effects (cow differences). rRNA. Taxon tables, as described above were subject to differential gene expression analysis following the same workflow as described for the SEED functions.

Quantification of mRNA and rRNA transcripts per gram rumen fluid. We quantified mRNA and rRNA transcripts per gram rumen fluid as follows:

$$transcriptA = totalRNA \times \frac{xRNA_r}{xRNA_r + yRNA_r} \times \frac{transcript\ A_r}{xRNAsubsample_r} \times \frac{N_A}{M(Nt) \times transcript\ A_{length}} \quad (1)$$

where *totalRNA* is the amount of RNA [µg] extracted per gram rumen fluid, $xRNA_r$, $yRNA_r$ and $xRNAsubsample_r$ are the number of reads of m/rRNA, r/mRNA and m/rRNA subsample used for functional annotation or taxonomic classification, respectively. $transcriptA_r$ and $transcriptA_{length}$ are the number of reads assigned to a certain transcript and the length of the particular transcript. N_A is the Avogadro constant and *M(Nt)* is the average molecular weight of a ssDNA nucleotide (330×10^6 µg mol^{-1}). For the transcript lengths we used average values of 1000 and 1500/1900 (prokaryotes/eukaryotes) nucleotides for mRNA and rRNA transcripts, respectively. As previously observed [70] the polyadenylation during cDNA synthesis is moderately enriching mRNA, therefore a ratio of mRNA:totalRNA reads of 1:25 was used to calculate transcript numbers per gram rumen fluid, as this ratio was observed in a previous study on the rumen microbiome of cows from the same

508 breed, housed at the same facility, fed a diet containing similar amounts of neutral detergent fibre,
509 crude protein and fat [24].
510

511 ## Declarations

512 **Ethics approval and consent to participate**. The animal experiments were approved by The
513 Experimental Animal Inspectorate under The Danish Ministry of Justice (journal no. 2008/561-1500).
514 **Consent for publication**. Not applicable.
515 **Availability of data and material.** Raw sequence data have been submitted to the NCBI Sequence
516 Read Archive (SRA) under the accession numbers SAMN07313968 - SAMN07313983.
517 **Competing interests**. The authors declare that they have no competing interests.
518 **Funding**. A.S. was financially supported by a scholarship of the University of Vienna for doctoral
519 candidates (uni:docs), a travel scholarship of the University of Vienna (KWA) and a scholarship by the
520 OeAD (Austrian agency for international mobility and cooperation in education, science and
521 research) for doctoral candidates (Marietta-Blau-Fellowship). T.U acknowledges financial support
522 from the University of Greifswald.
523 **Authors' contributions**. The study was designed by M.P., A.S. and T.U. Samples were collected by
524 M.P. Gas and VFA quantifications were established and performed by M.P. AL.H. and P.L. RNA
525 extractions and sample preparation were performed by A.S. Analysis of Illumina sequencing data
526 were performed by A.S., AT.T. and T.U. Statistical analyses and figures were done by A.S. and J.B,
527 assisted by M.B. and AT.T. The manuscript was written by A.S. and T.U., assisted by all co-authors.
528 **Acknowledgements**. We thank Thomas Rattei (University of Vienna) for bioinformatics support and
529 Andreas Sommer and the Vienna Biocenter Next Generation Sequencing Facility (www.vbcf.ac.at) for
530 library preparation and sequencing.
531

532 ## References

533 1. Hungate RE. The rumen microbial ecosystem. Annu Rev Ecol Evol Syst. 1975;6:39-66.

534 2. IPCC Core Writing Team, Pachauri RK & Meyer LA, editors. Climate Change 2014: Synthesis
535 Report. Contribution of Working Groups I, II and III to the Fifth Assessment Report of the
536 Intergovernmental Panel on Climate Change. Geneva: IPCC; 2014.
537 3. Hofmann RR. Evolutionary steps of ecophysiological adaptation and diversification of ruminants:
538 a comparative view of their digestive system. Oecologia 1989;78:443-457.
539 4. Bergman EN. Energy contributions of volatile fatty acids from the gastrointestinal tract in various
540 species. Physiol rev. 1990;70:567-90.
541 5. Johnson KA, Johnson DE. Methane emissions from *cattle. J* Anim Sci. 1995;73:2483-92.
542 6. Stocker TF, Qin D, Plattner G-K, Tignor M, Allen SK, Boschung J, Nauels A, Xia Y, Bex V, Midgley
543 PM, editors. Climate Change 2013: The Physical Science Basis. Contribution of Working Group I to
544 the Fifth Assessment Report of the Intergovernmental Panel on Climate Change. Cambridge:
545 Cambridge University Press; 2013.
546 7. Alexandratos N, Bruinsma J. World agriculture towards 2030/2050: the 2012 revision. Food and
547 Agriculture Organization of the United Nations (FAO) 2012.
548 8. Kumar S, Choudhury PK, Carro MD, Griffith GW, Dagar SS, Puniya M et al. New aspects and
549 strategies for methane mitigation from ruminants. Appl Microbiol Biotechnol. 2014;98:31-44.
550 9. Gruby D, Delafond HMO. Recherches sur des animalcules se développant en grand nombre dans
551 l'estomac et dans les intestins, pendant la digestion des animaux herbivores et carnivores. Compt
552 rend acad sci. 1843;17:1304-1308.
553 10. Hungate RE. Studies on cellulose fermentation: III. The culture and isolation for cellulose-
554 decomposing bacteria from the rumen of cattle. J bacteriol. 1947;53:631.
555 11. Hungate RE. I. Microbial ecology of the rumen. Bacteriol rev. 1960;24:353–364.
556 12. Orpin CG. Studies on the rumen flagellate Neocallimastix frontalis. J Gen Microbiol. 1975;91:249-
557 62.

13. Henderson G, Cox F, Ganesh S, Jonker A, Young W, Global Rumen Census Collaborators *et al*. Rumen microbial community composition varies with diet and host, but a core microbiome is found across a wide geographical range. Sci Rep. 2015;5:14567.

14. Wallace RJ, Snelling TJ, McCartney CA, Tapio I, Strozzi F. Application of meta-omics techniques to understand greenhouse gas emissions originating from ruminal metabolism. Genet Sel Evol. 2017;49:9.

15. Kittelmann S, Pinares-Patiño CS, Seedorf H, Kirk MR, Ganesh S, McEwan JC *et al*. Two different bacterial community types are linked with the low-methane emission trait in sheep. PLoS ONE 2014;9:e103171.

16. Shi W, Moon CD, Leahy SC, Kang D, Froula J, Kittelmann S *et al*. Methane yield phenotypes linked to differential gene expression in the sheep rumen microbiome. Genome Res. 2014;24:1517-1525.

17. Jeyanathan J, Kirs M, Ronimus R, Hoskin S, Janssen P. Methanogen community structure in the rumens of farmed sheep, cattle and red deer fed different diets. FEMS Microbiol Ecol. 2011;76:311-326.

18. Sun X, Henderson G, Cox F, Molano G, Harrison SJ, Luo D *et al*. Lambs fed fresh winter forage rape (*Brassica napus* L.) emit less methane than those fed perennial ryegrass (*Lolium perenne* L.), and possible mechanisms behind the difference. PLoS ONE 2015;10:e0119697.

19. Hristov AN, Oh J, Firkins JL, Dijkstra J, Kebreab E, Waghorn G *et al.* Special topics - Mitigation of methane and nitrous oxide emissions from animal operations: I. A review of enteric methane mitigation options. J Anim Sci. 2013;91:5045-5069.

20. Dai X, Tian Y, Li J, Luo Y, Liu D, Zheng H *et al*. Metatranscriptomic analyses of plant cell wall polysaccharide degradation by microorganisms in the cow rumen. Appl Environ Microbiol. 2015;81:1375-1386.

582 21. Comtet-Marre S, Parisot N, Lepercq P, Chaucheyras-Durand F, Mosoni P, Peyretaillade E *et al*.
583 Metatranscriptomics reveals the active bacterial and eukaryotic fibrolytic communities in the
584 rumen of dairy cow fed a mixed diet. Front Microbiol. 2017;8:67.
585 22. Hess M, Sczyrba A, Egan R, Kim TW, Chokhawala H, Schroth G *et al*. Metagenomic discovery of
586 biomass-degrading genes and genomes from cow rumen. Science 2011;331:463-467.
587 23. Patra AK. Enteric methane mitigation technologies for ruminant livestock: a synthesis of current
588 research and future directions. Environ Monit Assess. 2012;184:1929-52.
589 24. Poulsen M, Schwab C, Jensen BB, Engberg RM, Spang A, Canibe N *et al*. Methylotrophic
590 methanogenic Thermoplasmata implicated in reduced methane emissions from bovine rumen.
591 Nat Commun. 2013;4:1428.
592 25. Van Lingen HJ, Edwards JE, Vaidya JD, van Gastelen S, Saccenti E, van den Bogert B *et al*. Diurnal
593 dynamics of gaseous and dissolved metabolites and microbiota composition in the bovine
594 rumen. Front Microbiol. 2017;8:425.
595 26. Patra AK, Park T, Kim M, Yu Z. Rumen methanogens and mitigation of methane emission by anti-
596 methanogenic compounds and substances. J Anim Sci Biotechnol. 2017;8:13.
597 27. Li F, Henderson G, Sun X, Cox F, Janssen PH, Guan le L. Taxonomic assessment of rumen
598 microbiota using total RNA and targeted amplicon sequencing approaches. Front Microbiol.
599 2016;7:987.
600 28. Urich T, Lanzén A, Qi J, Huson DH, Schleper C, Schuster SC. Simultaneous assessment of soil
601 microbial community structure and function through analysis of the meta-transcriptome. PLoS
602 ONE 2008;3:e2527.
603 29. Geisen S, Tveit AT, Clark IM, Richter A, Svenning MM, Bonkowski M *et al*. Metatranscriptomic
604 census of active protists in soils. ISME J. 2015;9:2178-2190.
605 30. Eadie JM. Inter-relationships between certain rumen ciliate protozoa. J gen Microbiol.
606 1962;29:579-588.
607 31. Schimel J. Microbial ecology: Linking omics to biogeochemistry. Nat Microbiol. 2016;27:15028.

608 32. Kong Y, Teather R. Forster R. Composition, spatial distribution, and diversity of the bacterial
609 communities in the rumen of cows fed different forages. FEMS Microbiol Ecol. 2010;74:612-22.
610 33. Michalet-Doreau B, Fernandez I, Peyron C, Millet L, Fonty G. Fibrolytic activities and cellulolytic
611 bacterial community structure in the solid and liquid phases of rumen contents. Reprod Nutr
612 Dev. 2001;41:187-94.
613 34. Flint HJ, Scott KP, Duncan SH, Louis P, Forano E. Microbial degradation of complex carbohydrates
614 in the gut. Gut Microbes 2012;3:289-306.
615 35. Williams AG, Coleman GS. The rumen protozoa. In: Hobson PN, Stewart CS, editors. The rumen
616 microbial ecosystem. Netherlands: Springer; 1997. p 73-139.
617 36. Ben David Y, Dassa B, Borovok I, Lamed R, Koropatkin NM, Martens EC *et al*. Ruminococcal
618 cellulosome systems from rumen to human. Environ Microbiol. 2015;17:3407-3426.
619 37. Söllinger A, Schwab C, Weinmaier T, Loy A, Tveit AT, Schleper C *et al*. Phylogenetic and genomic
620 analysis of Methanomassiliicoccales in wetlands and animal intestinal tracts reveals clade-specific
621 habitat preferences. FEMS Microbiol Ecol. 2016;92:fiv149.
622 38. Paul K, Nonoh J, Mikulski L, Brune A. 'Methanoplasmatales,' Thermoplasmatales-Related Archaea
623 in termite guts and other environments, are the seventh order of methanogens. Appl Environ
624 Microbiol. 2012;78:8245-8253.
625 39. Lueders T, Chin KJ, Conrad R, Friedrich M. Molecular analyses of methyl-coenzyme M reductase
626 alpha-subunit (mcrA) genes in rice field soil and enrichment cultures reveal the methanogenic
627 phenotype of a novel archaeal lineage. Environ Microbiol. 2001;3:194-204.
628 40. Lang K, Schuldes J, Klingl A, Poehlein A, Daniel R, Brune A. New mode of energy metabolism in
629 the seventh order of methanogens as revealed by comparative genome analysis of 'Candidatus
630 Methanoplasma termitum'. Appl Environ Microbiol. 2015;81:1338-1352.
631 41. Borrel G, Parisot N, Harris HM, Peyretaillade E, Gaci N, Tottey W *et al*. Comparative genomics
632 highlights the unique biology of Methanomassiliicoccales, a Thermoplasmatales-related seventh
633 order of methanogenic archaea that encodes pyrrolysine. BMC Genomics 2014;15:679.

634 42. Liu Y, Whitman W. Metabolic, phylogenetic, and ecological diversity of the methanogenic
635 Archaea. Ann N Y Acad Sci. 2008;1125:171-189.
636 43. Gifford SM, Sharma S, Rinta-Kanto JM, Moran MA. Quantitative analysis of a deeply sequenced
637 marine microbial metatranscriptome. *ISME J.* 2011;5:461-472.
638 44. Moran MA, Satinsky B, Gifford SM, Luo H, Rivers A. Sizing up metatranscriptomics. *ISME J.*
639 2013;7:237-243.
640 45. Weimer PJ. Redundancy, resilience, and host specificity of the ruminal microbiota: implications
641 for engineering improved ruminal fermentations. Front Microbiol. 2015;6:296.
642 46. Li X, Højberg O, Canibe N, Jensen BB. Phylogenetic diversity of cultivable butyrate-producing
643 bacteria from pig gut content and feces. J Anim Sci. 2016;94:377-381.
644 47. Reichardt N, Duncan SH, Young P, Belenguer A, McWilliam Leitch C, Scott KP *et al.* Phylogenetic
645 distribution of three pathways for propionate production within the human gut microbiota. ISME
646 J. 2014;8:1323-35.
647 48. Janssen P, Kirs M. Structure of the Archaeal Community of the Rumen. Appl Environ Microb.
648 2008;74:3619-3625.
649 49. Tapio I, Snelling TJ, Strozzi F, Wallace RJ. The ruminal microbiome associated with methane
650 emissions from ruminant livestock. J Anim Sci Biotechnol. 2017;8:7.
651 50. Duin EC, Wagner T, Shima S, Prakash D, Cronin B, Yáñez-Ruiz DR *et al.* Mode of action uncovered
652 for the specific reduction of methane emissions from ruminants by the small molecule 3-
653 nitrooxypropanol. Proc Natl Acad Sci U S A. 2016;113:6172-6177.
654 51. Soliveres S, van der Plas F, Manning P, Prati D, Gossner MM, Renner SC *et al.* Biodiversity at
655 multiple trophic levels is needed for ecosystem multifunctionality. *Nature*
656 2016;25,536(7617):456-9.
657 52. Hellwing AL, Lund P, Weisbjerg MR, Brask M, Hvelplund T. Technical note: Test of a low cost and
658 animal-friendly system for measuring methane emissions from dairy cows. J Dairy Sci.
659 2012;95:6077-6085.

660 53. Petersen SO, Hellwing AL, Brask M, Højberg O, Poulsen M, Zhu Z *et al*. Dietary nitrate for
661 methane mitigation leads to nitrous oxide emissions from dairy cows. J Environ Qual.
662 2015;44:1063-1070.
663 54. Canibe N, Højberg O, Badsberg JH, Jensen BB. Effect of feeding fermented liquid feed and
664 fermented grain on gastrointestinal ecology and growth performance in piglets. J Anim Sci.
665 2007;85:2959-71.
666 55. Griffiths RI, Whiteley AS, O'Donnell AG, Bailey MJ. Rapid method for coextraction of DNA and
667 RNA from natural environments for analysis of ribosomal DNA-and rRNA-based microbial
668 community composition. Appl Environ Microbiol. 2000;66:5488-5491.
669 56. Schmieder R & Edwards R. Quality control and preprocessing of metagenomic datasets.
670 Bioinformatics 2011;27:863-4.
671 57. Kopylova E, Noé L & Touzet H. SortMeRNA: fast and accurate filtering of ribosomal RNAs in
672 metatranscriptomic data. Bioinformatics 2012;28:3211-3217.
673 58. Lanzén A, Jørgensen SL, Huson DH, Gorfer M, Grindhaug SH, Jonassen I *et al*. CREST–classification
674 resources for environmental sequence tags. PloS ONE 2012;7:e49334.
675 59. Huson DH, Mitra S, Ruscheweyh H-J, Weber N, Schuster SC. Integrative analysis of environmental
676 sequences using MEGAN4. Genome Res. 2011;21:1552-1560.
677 60. R Core Team. R: A language and environment for statistical computing. R Foundation for
678 Statistical Computing. 2013; Vienna, Austria.
679 61. McCarthy DJ, Chen Y & Smyth GK. Differential expression analysis of multifactor RNA-Seq
680 experiments with respect to biological variation. Nucleic Acids Res. 2012;40:4288-97.
681 62. Oksanen J *et al*. vegan: Community Ecology Package. R package version 2.3-4. 2016.
682 https://CRAN.R-project.org/package=vegan.
683 63. De Cáceres M & Legendre P. Associations between species and groups of sites: indices and
684 statistical inference. Ecology 2009;90:3566-74.

64. Zhao S, Guo Y, Sheng Q & Shyr Y. Heatmap3: an improved heatmap package with more powerful and convenient features. BMC Bioinformatics 2014;15:P16.

65. Buchfink B, Xie C, Huson D. Fast and sensitive protein alignment using DIAMOND. Nat Methods 2015;12:59-60.

66. Finn R, Bateman A, Clements J, Coggill P, Eberhardt RY, Eddy SR *et al*. Pfam: the protein families database. Nucleic Acids Res. 2014;42:D222-D230.

67. Tveit A, Urich T, Frenzel P & Svenning M. Metabolic and trophic interactions modulate methane production by Arctic peat microbiota in response to warming. *Proc Natl Acad Sci USA.* 2015;112:E2507-E2516.

68. Louis P & Flint HJ. Diversity, metabolism and microbial ecology of butyrate-producing bacteria from the human large intestine. FEMS Microbiol Lett. 2009;294:1-8.

69. Vital M, Howe AC & Tiedje JM. Revealing the bacterial butyrate synthesis pathways by analyzing (meta) genomic data. MBio 2014;5:e00889-14.

70. Frias-Lopez J *et al.* Microbial community gene expression in ocean surface waters. Proc Natl Acad Sci USA. 2008;105:3805-3810.

Supplementary Information

Supplementary Information is provided in the PDF document "Supplementary_Figures_Tables.pdf". This Supplementary Information contains Figures and Tables supplementing the main manuscript.

Figure legends

Figure 1. Ruminant gas emissions and volatile fatty acid (VFA) production. (a) Overview of the animal feeding trial during twelve hours (4 am - 4 pm) of sampling; for more details see Methods section. (b) Carbon dioxide (CO_2), methane (CH_4) and hydrogen (H_2) emissions measured using open-circuit respiration chambers. (c), (d) Total VFA concentrations and total RNA content quantified per gram rumen fluid (RF). Colour code indicates the four rumen-cannulated Holstein dairy cows.

711 **Figure 2. Rumen microbiome community composition and temporal dynamics**. Three domain
712 profiles showing the overall rumen microbial community composition on phylum (a), class (b) and
713 family (c) level. Tile sizes are reflecting the average relative abundance of eukaryotic (green),
714 bacterial (blue) and archaeal (orange) taxa observed in the 16 rumen metatranscriptomes. (d) shows
715 the highly individual microbial communities within each cow over time. Taxa which could not be
716 assigned on family level and/or showed relative abundance ≤ 0.01 % level are shown on higher
717 taxonomic levels. All taxa detected in the rumen microbiomes and their relative abundances are
718 listed in Supplementary Table S4.
719
720 **Figure 3. Global functional response of rumen microbiome to ruminant feed intake**. Boxes showing
721 the mean relative abundance of SEED subsystem level 1 (a), SEED subsystem level 2 (b), SEED
722 subsystem level 3 (c) and SEED functions (c, small tiles) of eight rumen metatranscriptomes (t0 and t1
723 metatranscriptomes). Colour code indicates SEED subsystems containing functions that were
724 identified by differential gene expression analysis to be significantly higher expressed one hour after
725 the feeding (t1) compared to before the feeding (t0). The particular upregulated functions are
726 coloured in orange. All functions that were subject to differential gene expression analysis (1659
727 SEED functions) are depicted, low abundant transcripts were excluded. For more details on the
728 significantly higher expressed functions (e.g. functional assignment of the numbered tiles) see
729 Supplementary Table S5.
730 **Figure 4. Comparison of relative and quantified transcript abundance of methanogens.** Relative and
731 quantified transcript abundance of methanogenesis specific mRNA (upper boxplots) and SSU rRNA of
732 methanogens (lower boxplots) are depicted in (a) and (b), respectively. Data: mRNA reads assigned
733 to the SEED subsystem Methanogenesis and SSU rRNA reads assigned to methanogens were
734 summarized. For details on the quantification see Methods section and equation 1; x-axis: before
735 feeding (t0), one, three, five hours after feeding started (t1, t3, t5).
736

737 **Figure 5. Dynamics and distribution of carbohydrate active enzymes (CAZymes) among the rumen**
738 **microbiome**. Circles depict the quantified numbers of CAZyme transcripts (g^{-1} rumen fluid),
739 summarized in respective to their activity (cellulases, hemicellulases, starch degrading enzymes and
740 oligosaccharide hydrolases), separated for the major Bacteria and Eukarya involved in the breakdown
741 of complex plant material (on phylum level and lowest common dominant taxon). Colour code
742 indicate the different cows and the different time points (grey scale of the columns); before feeding
743 (t0), one, three, five hours after feeding started (t1, t3, t5).
744
745 **Figure 6. Methane and methanogen transcript dynamics during plant biomass degradation**. (a)
746 Methane emissions and quantified SSU rRNA transcripts of the two methanogen orders present in
747 the rumen metatranscriptomes, *Methanomassiliicoccales* and *Methanobacteriales* (i.e.
748 *Methanobrevibacter* and *Methanosphaera*), before feeding (t0) and one (t1), three (t3) and five (t5)
749 hours after the feeding started. (b) Quantified *mcr*A (functional marker for all methanogens)
750 transcripts. (c) Quantified *mtMA* (methylamine-specific methyltransferases) and *mtr*A transcripts
751 (methyl-H_4MPT:HS-CoM methyltransferase, alpha subunit), key transcripts in
752 *Methanomassiliicoccales* and *Methanobrevibacter* specific methanogenesis, respectively. *mtMA*
753 summarizes mono-, di- and trimethylamine-specific methyltransferase (*mtm*B, *mtb*B and *mtt*B)
754 transcripts, whereas *mtt*B transcripts constitute to > 70 % of the *mtMA* transcripts. (d) Quantified
755 *mta*B (methanol-specific methyltransferase) transcripts. *Methanomassiliicoccales* and
756 *Methanosphaera mta*B transcripts are negatively and positively correlating with CH_4 emissions,
757 respectively. Mean of the four cows is shown for each time-point, error bars depict standard error of
758 the mean (SEM). Asterisk indicate significant differences between the respective time-points and the
759 previous one (* $p < 0.5$, ** $p < 0.01$).

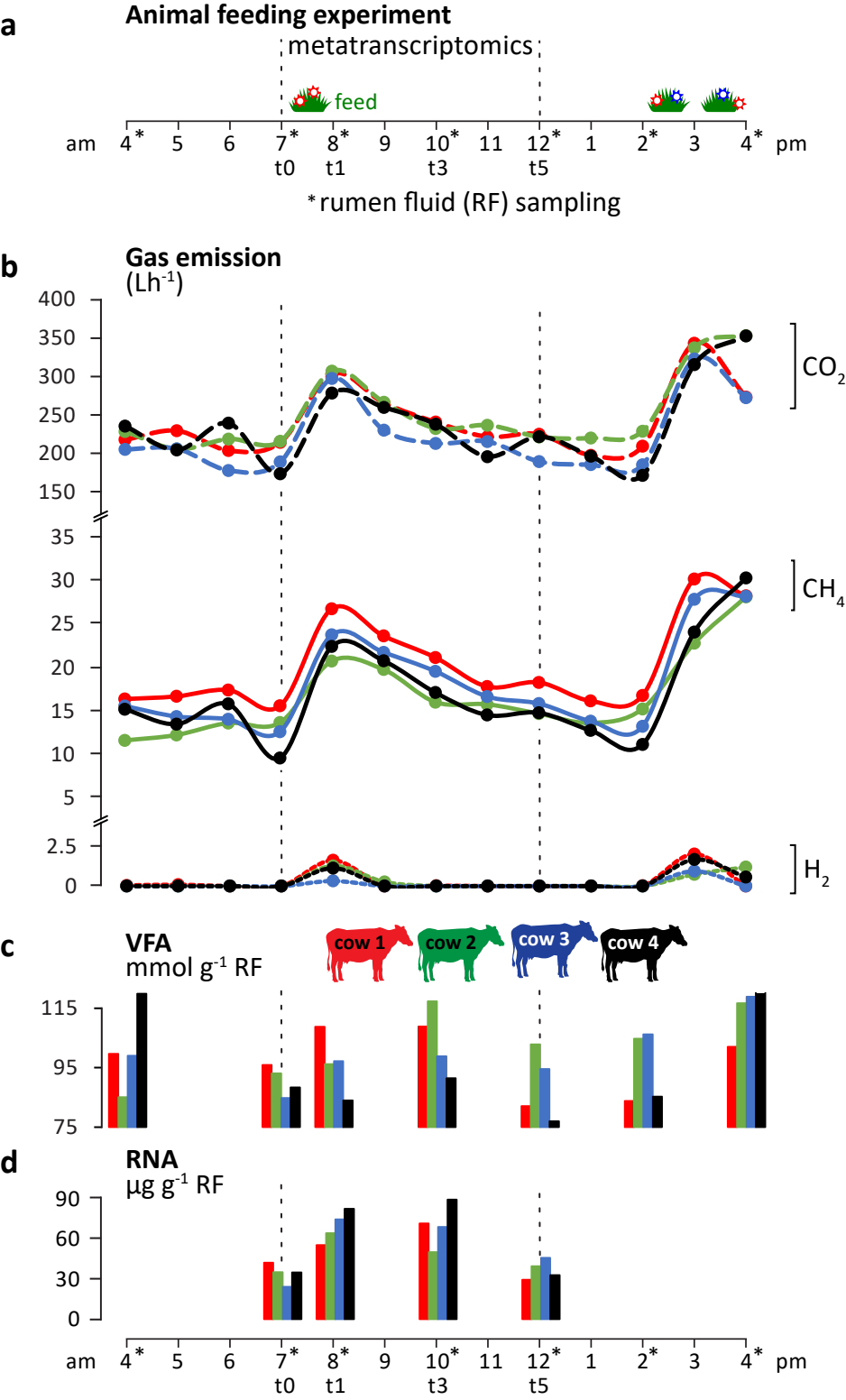
a
Animal feeding experiment
metatranscriptomics
feed
am
4*
5
6
7*
8*
9
10*
11
12*
1
2*
3
4*
pm
t0
t1
t3
t5
*rumen fluid (RF) sampling
b
Gas emission
(Lh-1)
400
350
300
250
200
150
CO2
35
30
25
20
15
10
5
CH4
2.5
0
H2
c
VFA
mmol g-1 RF
cow 1
cow 2
cow 3
cow 4
115
95
75
d
RNA
µg g-1 RF
90
60
30
0

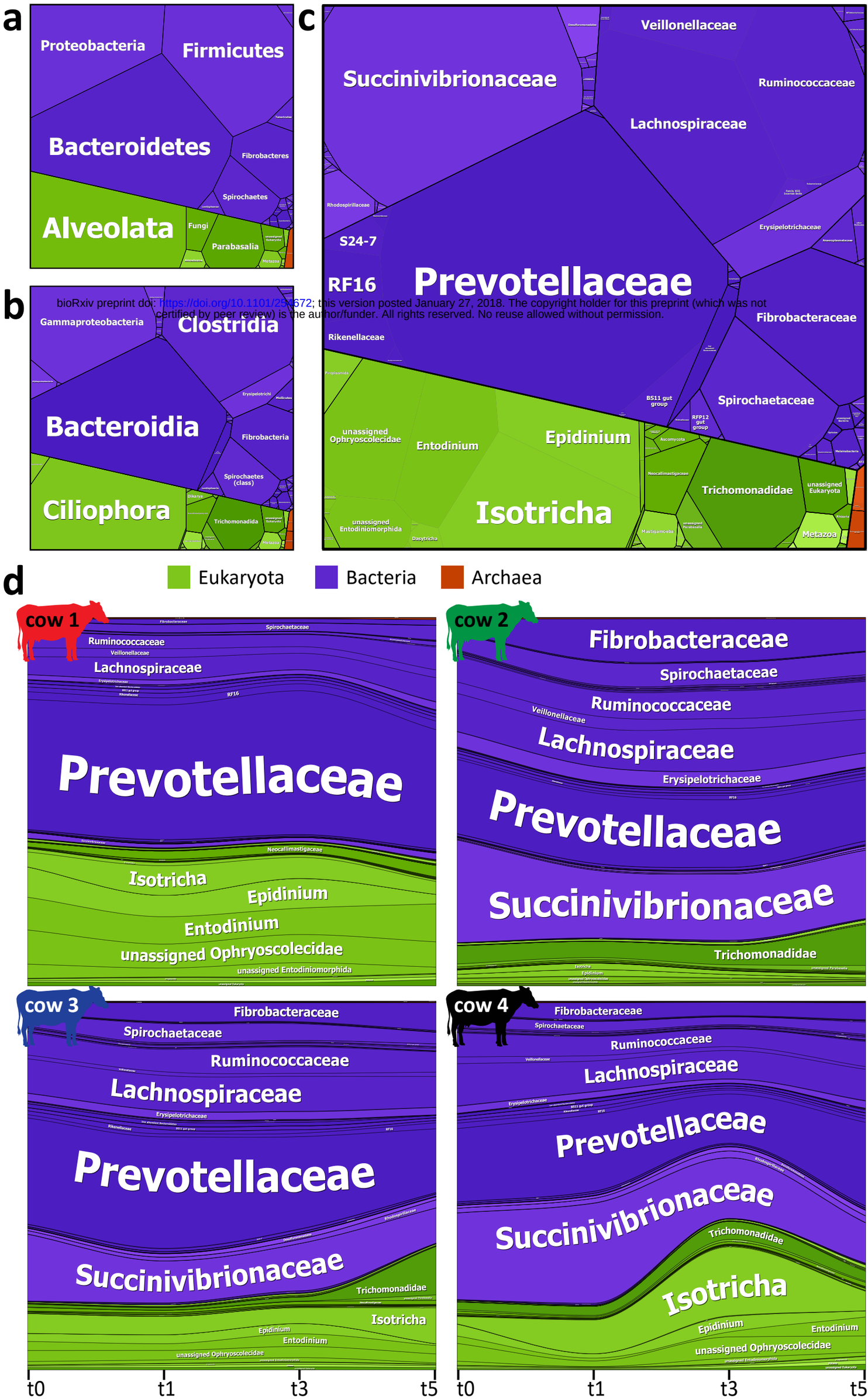

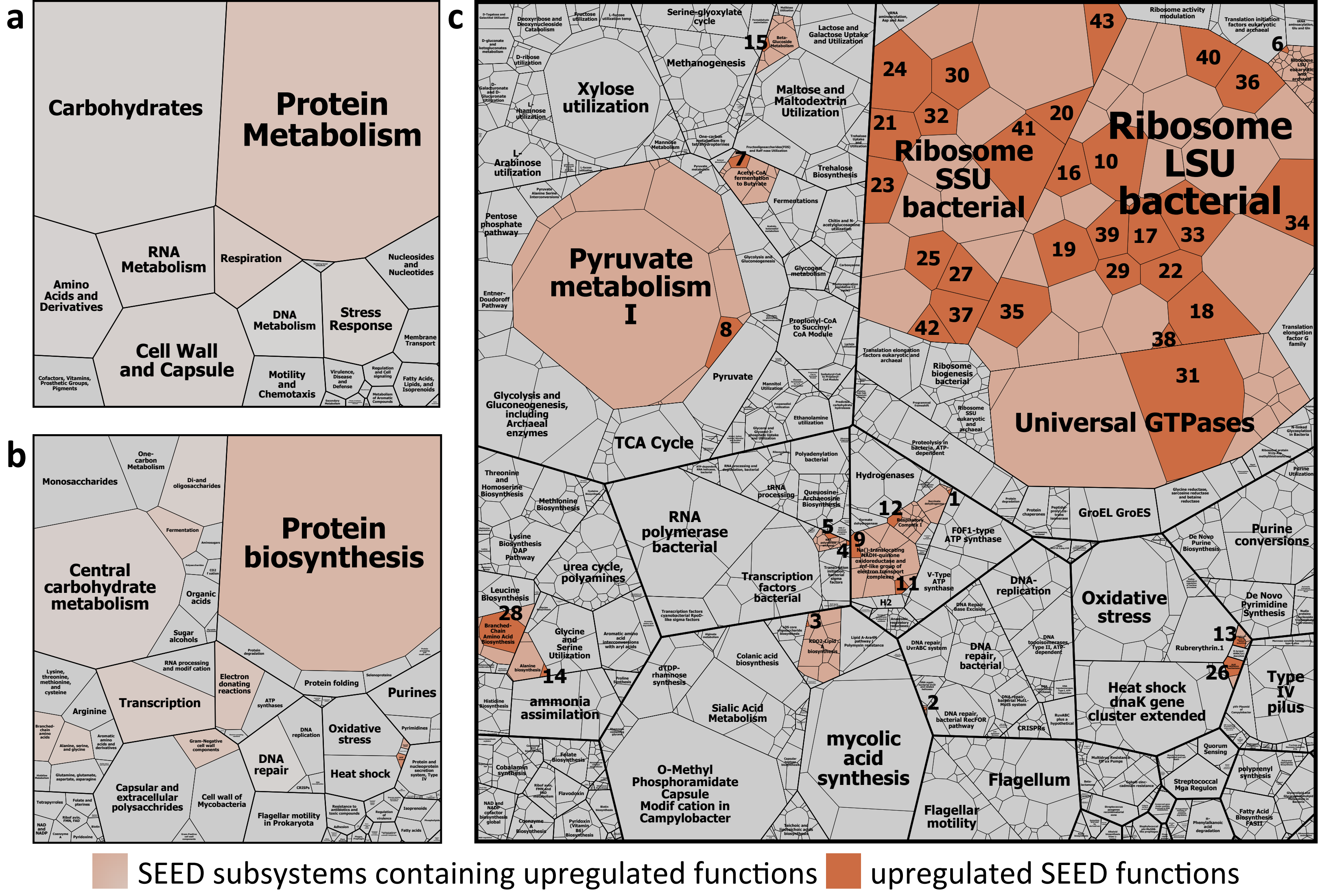

a
Carbohydrates
Protein Metabolism
RNA Metabolism
Respiration
Amino Acids and Derivatives
Nucleosides and Nucleotides
DNA Metabolism
Stress Response
Cell Wall and Capsule
Membrane Transport
Cofactors, Vitamins, Prosthetic Groups, Pigments
Motility and Chemotaxis
Virulence, Disease and Defense
Regulation and Cell signaling
Fatty Acids, Lipids, and Isoprenoids
Metabolism of Aromatic Compounds
Secondary Metabolism
b
Monosaccharides
One-carbon Metabolism
Di-and oligosaccharides
Protein biosynthesis
Fermentation
Aminosugars
Polysaccharides
CO2 f xation
Central carbohydrate metabolism
Organic acids
Sugar alcohols
Protein degradation
RNA processing and modif cation
Lysine, threonine, methionine, and cysteine
Electron donating reactions
Transcription
Arginine
Protein folding
Selenoproteins
Purines
ATP synthases
Branched-chain amino acids
Alanine, serine, and glycine
Aromatic amino acids and derivatives
Gram-Negative cell wall components
DNA replication
Oxidative stress
Pyrimidines
Histidine Metabolism
Glutamine, glutamate, aspartate, asparagine
DNA repair
Heat shock
Protein and nucleoprotein secretion system, Type IV
CRISPs
Tetrapyrroles
Folate and pterines
Capsular and extracellular polysacchrides
Cell wall of Mycobacteria
Resistance to antibiotics and toxic compounds
Regulation of virulence
Isoprenoids
Ribof avin, FMN, FAD
Flagellar motility in Prokaryota
Adhesion
NAD and NADP
Coenzyme A
Pyridoxine
Biotin
Fatty acids
Phages, Prophages
c
Xylose utilization
Methanogenesis
Serine-glyoxylate cycle
Deoxyribose and Deoxynucleoside Catabolism
Lactose and Galactose Uptake and Utilization
Maltose and Maltodextrin Utilization
Beta-Glucoside Metabolism
L-Arabinose utilization
Mannose Metabolism
One-carbon metabolism by tetrahydropterines
Acetyl-CoA fermentation to Butyrate
Trehalose Biosynthesis
Fermentations
Pentose phosphate pathway
Pyruvate metabolism I
Chitin and N-acetylglucosamine utilization
Glycolysis and Gluconeogenesis
Glycogen metabolism
Entner-Doudoroff Pathway
Propionyl-CoA to Succinyl-CoA Module
Pyruvate
Glycolysis and Gluconeogenesis, including Archaeal enzymes
TCA Cycle
Mannitol Utilization
Ethanolamine utilization
Ribosome SSU bacterial
Ribosome LSU bacterial
Ribosome activity modulation
Translation initiation factors eukaryotic and archaeal
Translation elongation factors eukaryotic and archaeal
Ribosome biogenesis bacterial
Ribosome SSU eukaryotic and archaeal
Universal GTPases
Translation elongation factor G family
N-linked Glycosylation in Bacteria
Proteolysis in bacteria, ATP-dependent
Hydrogenases
Polyadenylation bacterial
tRNA processing
Queuosine-Archaeosine Biosynthesis
Threonine and Homoserine Biosynthesis
Methionine Biosynthesis
RNA polymerase bacterial
Lysine Biosynthesis DAP Pathway
urea cycle, polyamines
Transcription factors bacterial
Transcription initiation, bacterial sigma factors
Respiratory Complex I
Na()-translocating NADH-quinone oxidoreductase and rnf-like group of electron transport complexes
F0F1-type ATP synthase
V-Type ATP synthase
H2
GroEL GroES
Protein chaperones
Purine conversions
De Novo Purine Biosynthesis
De Novo Pyrimidine Synthesis
Leucine Biosynthesis
Branched-Chain Amino Acid Biosynthesis
Alanine biosynthesis
Glycine and Serine Utilization
Aromatic amino acid interconversions with aryl acids
Transcription factors cyanobacterial RpoD-like sigma factors
KDO2-Lipid A biosynthesis
Lipid A-Ara4N pathway (Polymyxin resistance)
DNA-replication
Oxidative stress
Rubrerythrin.1
DNA repair, UvrABC system
DNA repair, bacterial
DNA topoisomerases, Type II, ATP-dependent
Histidine Biosynthesis
ammonia assimilation
dTDP-rhamnose synthesis
Colanic acid biosynthesis
Sialic Acid Metabolism
mycolic acid synthesis
DNA repair, bacterial RecFOR pathway
CRISPRs
Heat shock dnaK gene cluster extended
Type IV pilus
Cobalamin synthesis
Folate Biosynthesis
O-Methyl Phosphoramidate Capsule Modif cation in Campylobacter
Flagellum
Flagellar motility
Quorum Sensing
polyprenyl synthesis
Streptococcal Mga Regulon
Multidrug Resistance Eff ux Pumps
Fatty Acid Biosynthesis FASII
n-Phenylalkanoic acid degradation
NAD and NADP cofactor biosynthesis global
Coenzyme A Biosynthesis
Pyridoxin (Vitamin B6) Biosynthesis
Flavodoxin
Teichoic and lipoteichoic acids biosynthesis
1 2 3 4 5 6 7 8 9 10 11 12 13 14 15 16 17 18 19 20 21 22 23 24 25 26 27 28 29 30 31 32 33 34 35 36 37 38 39 40 41 42 43
SEED subsystems containing upregulated functions
upregulated SEED functions

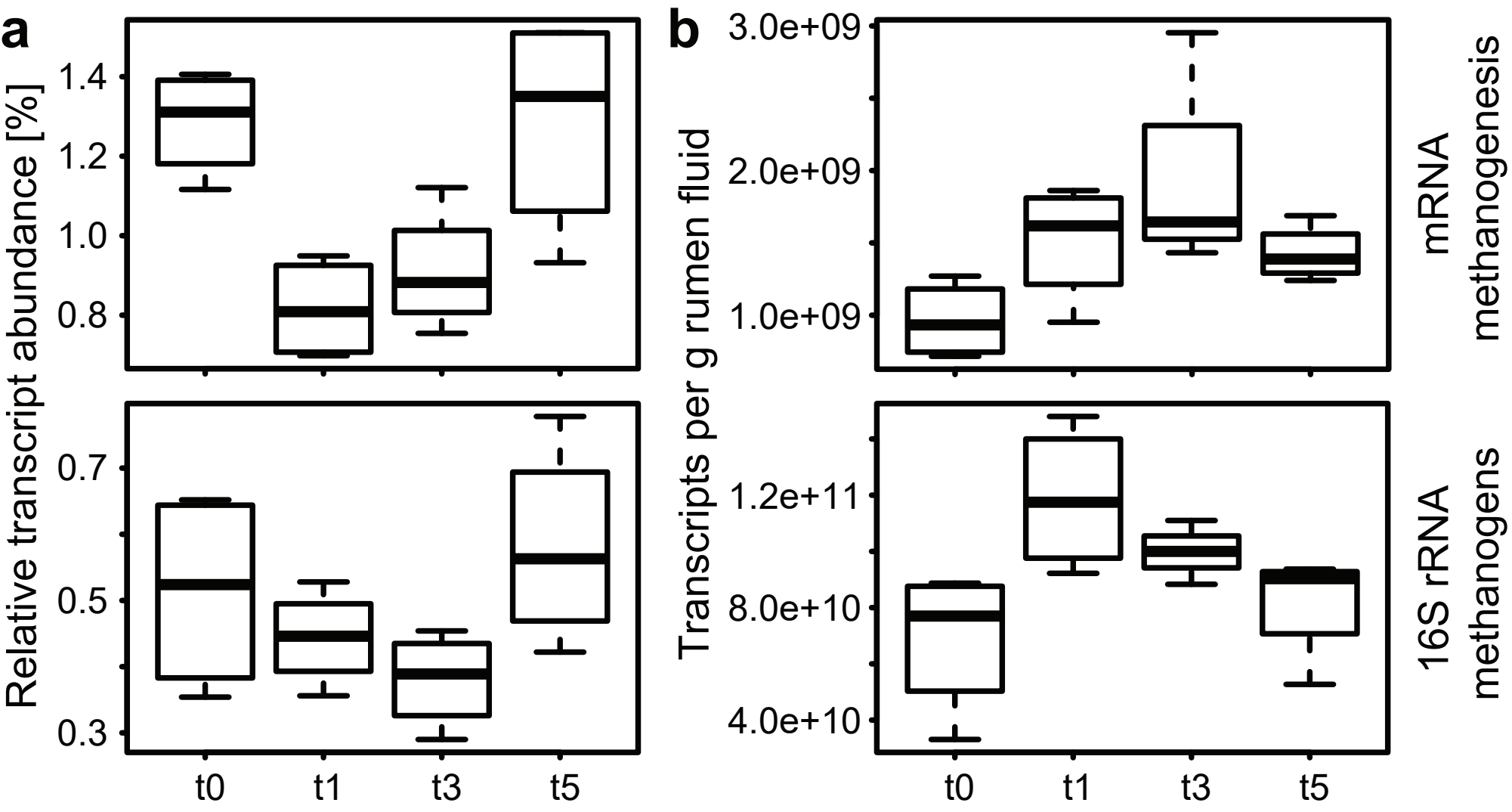
a
b
Relative transcript abundance [%]
1.4
1.2
1.0
0.8
0.7
0.5
0.3
Transcripts per g rumen fluid
3.0e+09
2.0e+09
1.0e+09
1.2e+11
8.0e+10
4.0e+10
mRNA
methanogenesis
16S rRNA
methanogens
t0
t1
t3
t5

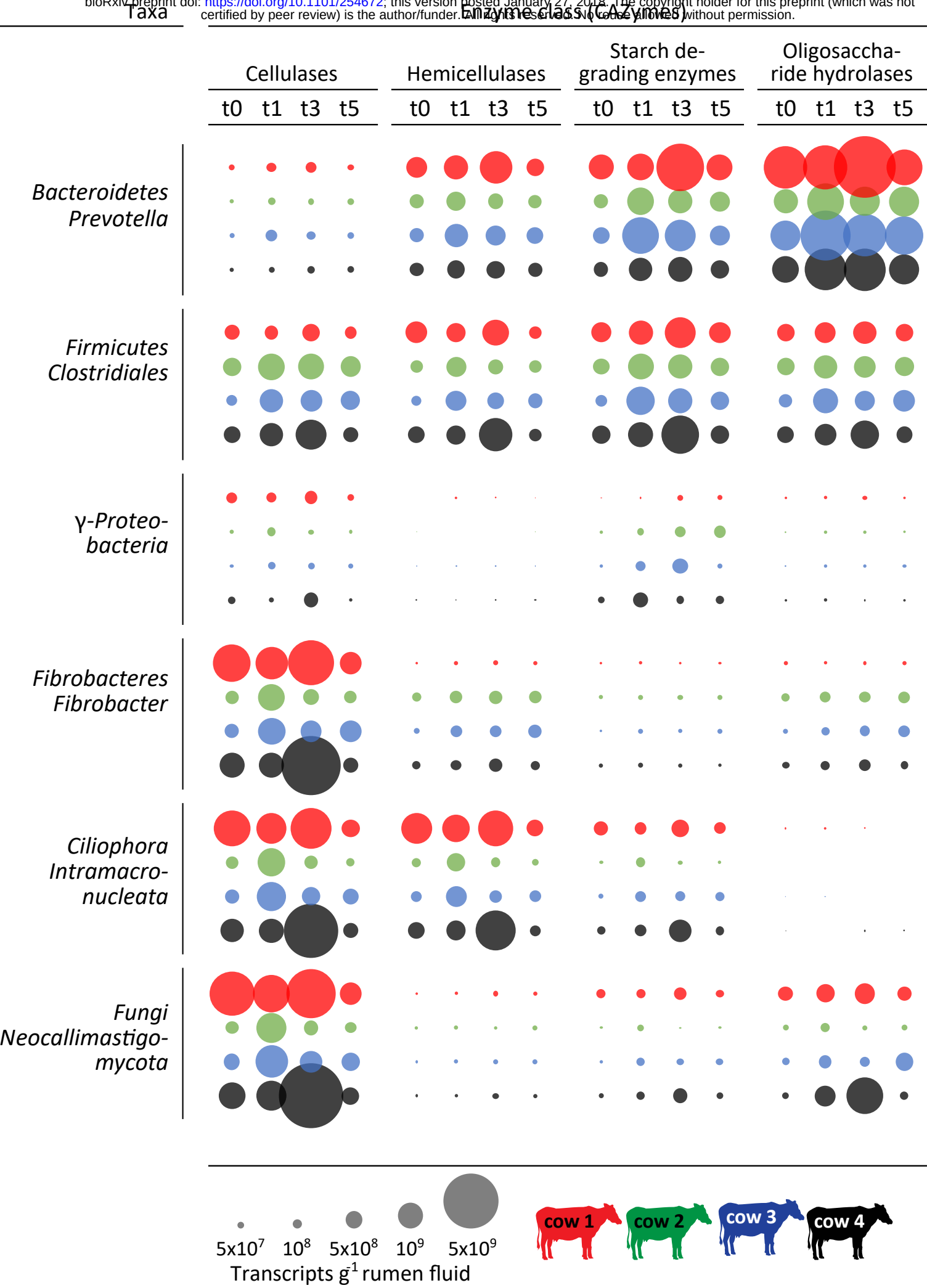

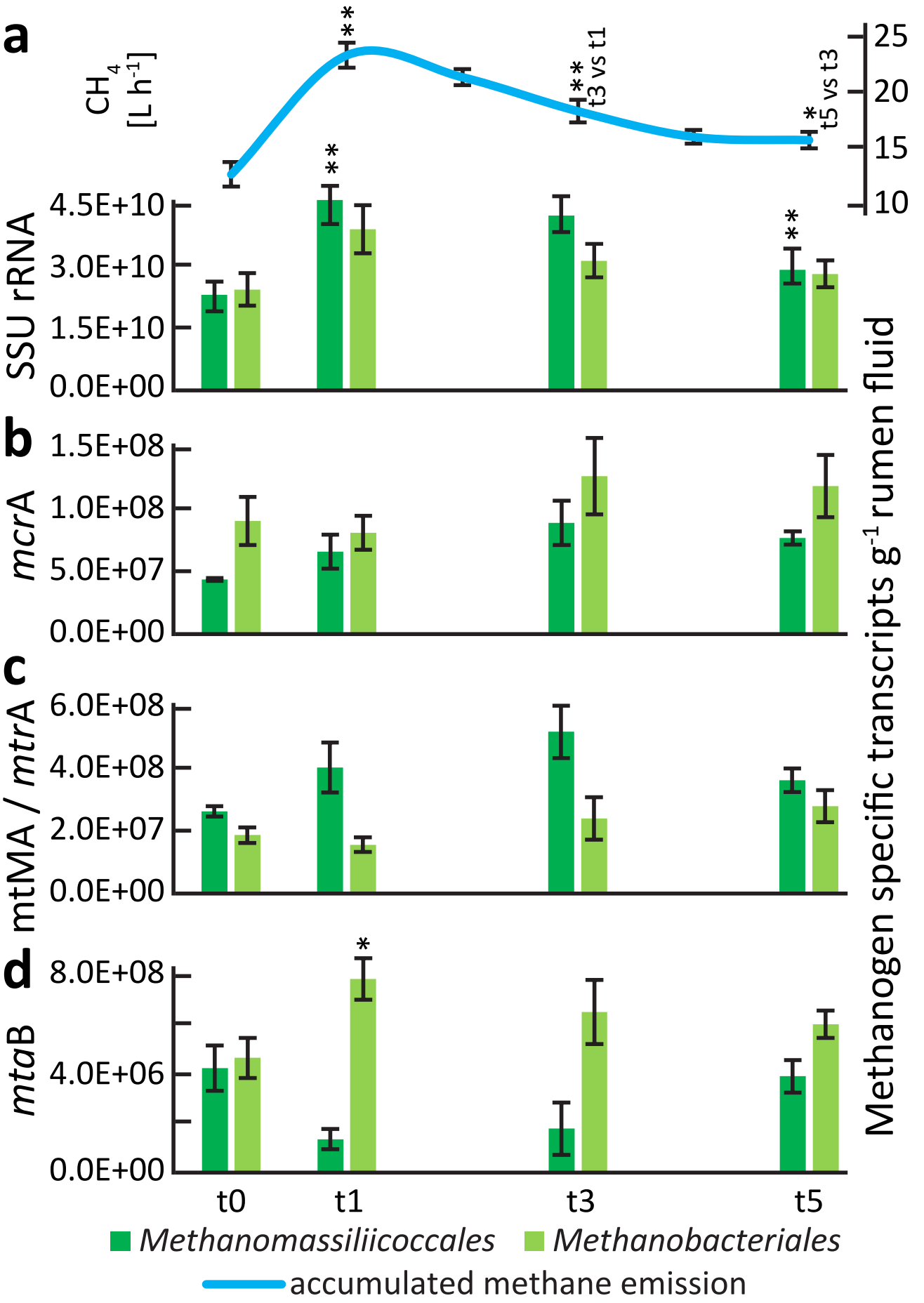
a
CH4 [L h-1]
25
20
15
10
**
**
t3 vs t1
*
t5 vs t3
SSU rRNA
4.5E+10
3.0E+10
1.5E+10
0.0E+00
**
b
mcrA
1.5E+08
1.0E+08
5.0E+07
0.0E+00
c
mtMA / mtrA
6.0E+08
4.0E+08
2.0E+07
0.0E+00
d
mtaB
8.0E+08
4.0E+06
0.0E+00
*
t0
t1
t3
t5
Methanomassiliicoccales
Methanobacteriales
accumulated methane emission
Methanogen specific transcripts g-1 rumen fluid